Half-metallic electronic structure of Co_2MnSi electrodes in fully epitaxial $Co_2MnSi/MgO/Co_2MnSi$ magnetic tunnel junctions investigated by tunneling spectroscopy (invited)

Takayuki Ishikawa, Naoki Itabashi, Tomoyuki Taira, Ken-ichi Matsuda, Tetsuya Uemura, and Masafumi Yamamoto[a)]
Division of Electronics for Informatics, Hokkaido University, Sapporo 060-0814, Japan

(Presented 12 November 2008; received 22 September 2008; accepted 8 February 2009; published online 30 March 2009)

We used tunneling spectroscopy to examine the spin-dependent electronic structure of Co_2MnSi (CMS) electrodes facing a MgO barrier and the key tunneling mechanism in fully epitaxial CMS/MgO/CMS magnetic tunnel junctions (MTJs) that showed high tunnel magnetoresistance ratios up to 182% at room temperature and 705% at 4.2 K. Consequently, we developed a model of the spin-dependent electronic structure for CMS electrodes and a tunneling model that can consistently explain the observed tunneling spectra. Here, we show that lower (upper) CMS electrodes possess a half-metal gap of 0.40 eV (0.32 eV) with the Fermi level (E_F) near the middle of the half-metal gap for both lower and upper CMS electrodes. Furthermore, we found strong evidence for the existence of interface states in the interfacial region of CMS electrodes facing a MgO barrier, as well as evidence of residual states in the bulk region of upper CMS electrodes, in both cases for minority spins around E_F, and we show that interface states play a critical role for spin-dependent tunneling in these half-metallic CMS-based MTJs. © *2009 American Institute of Physics*.
[DOI: 10.1063/1.3089732]

I. INTRODUCTION

The creation of a highly spin-polarized current is requisite for spintronic devices, in which both the charge and the spin of the electron are utilized as the information carrier.[1] Half-metallic ferromagnets[2] that are characterized by a 100% spin polarization at the Fermi level (E_F) are the most preferable ferromagnetic electrode materials for these devices. Recently, Co-based full-Heusler alloys (Co_2YZ) have attracted much interest as ferromagnetic electrodes[3–12] because of the half-metallic nature theoretically predicted for many of these alloys[13–15] and because of their high Curie temperatures, which are well above room temperature (RT).[16] Relatively high tunnel magnetoresistance (TMR) ratios up to 220% at RT have been demonstrated for magnetic tunnel junctions (MTJs) with a Co_2YZ electrode or Co_2YZ electrodes, including Co_2MnSi,[3,4,6,10,11] $Co_2Cr_{0.6}Fe_{0.4}Al$,[7] Co_2MnGe,[8] and $Co_2FeAl_{0.5}Si_{0.5}$ (Ref. 5). One Co-based full-Heusler alloy, in particular Co_2MnSi (CMS), has attracted interest because of its theoretically predicted half-metallic nature, with a large energy gap of 0.42 eV (Ref. 13) to 0.81 eV (Ref. 14) for its minority-spin band, and because of its high Curie temperature of 985 K.[16] Sakuraba *et al.*[4] reported a high TMR ratio of 570% at 2 K for CMS/AlO_x/CMS MTJs indicating an intrinsically high spin polarization of CMS but showed a relatively low TMR ratio of 67% at RT. Chioncel *et al.*[17] attributed this strong temperature (T) dependence of the TMR ratio observed for CMS/AlO_x/CMS MTJs to a strong T dependence of the CMS spin polarization arising from so called nonquasiparticle states. Mavropoulos *et al.*[18] pointed out, based on theoretical arguments, the crucial role of the interface states of half-metallic electrodes facing a tunnel barrier for spin-dependent tunneling in half-metal-based MTJs.

We developed fully epitaxial Heusler alloy-based MTJs with a MgO (001) tunnel barrier.[6–10] The relatively small lattice mismatch between Co_2YZ and MgO for a 45° in-plane rotation (−3.7% for $Co_2Cr_{0.6}Fe_{0.4}Al$ and −5.1% for CMS) within the (001) plane enabled us to successfully fabricate fully epitaxial MTJ trilayers featuring extremely smooth and abrupt interfaces.[6,7,9] Based on this device technology of Heusler alloy/MgO-based fully epitaxial MTJs, we recently fabricated fully epitaxial MTJs with CMS as both lower and upper electrodes and with a MgO barrier (CMS/MgO/CMS MTJs), and showed high TMR ratios of 179% at RT and 683% at 4.2 K.[10]

Our purpose in the current study has been to investigate the spin-dependent electronic structure of CMS electrodes facing a MgO barrier in CMS/MgO/CMS MTJs through tunneling spectroscopy. A second purpose has been to clarify the key tunneling mechanism in these fully epitaxial MTJs with potentially half-metallic electrodes.

In Sec. II, we describe our experimental method. In Sec. III, we first present experimental results regarding structural properties of CMS/MgO/CMS MTJ layer structures, and then we describe the dI/dV versus V and d^2I/dV^2 versus V characteristics of fabricated MTJs along with the TMR characteristics. We discuss these experimental results in Sec. IV in terms of the spin-dependent electronic structure of CMS electrodes and the key tunneling mechanism that determines

[a)]Author to whom correspondence should be addressed: Electronic mail: yamamoto@nano.ist.hokudai.ac.jp.

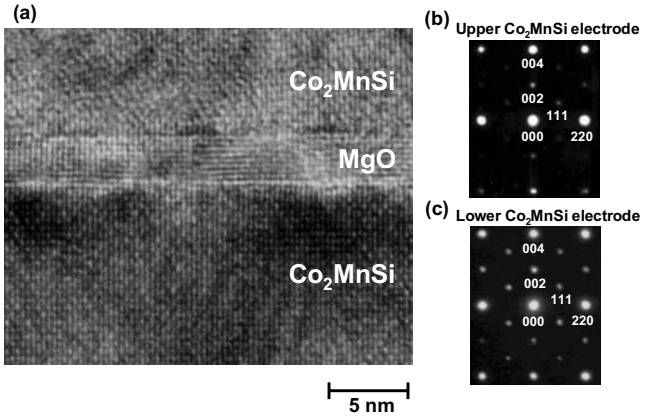

FIG. 1. (a) Cross-sectional high-resolution transmission electron microscope lattice image of a CMS (50 nm)/MgO (2.0 nm)/CMS (5 nm) MTJ layer structure along the [110] direction of the CMS layers. The MTJ layer structure was *in situ* annealed at 550 °C just after deposition of the upper CMS electrode. (b) Electron diffraction pattern for the upper CMS electrode (5 nm). The electron-beam diameter was 2.5 nm. (c) Electron diffraction pattern for the lower CMS electrode (50 nm). The electron-beam diameter was 15 nm.

the spin-dependent tunneling characteristics in fully epitaxial CMS/MgO/CMS MTJs. In Sec. V, we summarize our results and conclude.

II. EXPERIMENTAL

The fabricated MTJ layer structure was as follows: (from the substrate side) MgO buffer (10 nm)/CMS lower electrode (50 nm)/MgO tunnel barrier (2–3 nm)/CMS upper electrode (5 nm)/Ru (0.8 nm)/$Co_{90}Fe_{10}$ (2 nm)/IrMn (10 nm)/Ru cap (5 nm) grown on a MgO(001) substrate. The preparation of the CMS/MgO/CMS MTJ layer structure and the successive microfabrication of MTJs are described in detail elsewhere.[10] In brief, the CMS lower electrode was deposited at RT and subsequently annealed at 600 °C. The upper CMS electrode was deposited at RT. The MTJ layer structure was annealed *in situ* at several annealing temperatures (T_a) just after deposition of the upper electrode. The film composition for CMS electrodes used in this study was determined to be $Co_{2.0}Mn_{0.91}Si_{0.93}$ by inductively coupled plasma optical emission spectroscopy. The fabricated junction size was $10 \times 10\ \mu m^2$. We measured the differential conductance ($G = dI/dV$) versus V characteristics of the fabricated MTJs with a conventional lock-in method at 4.2 K. The modulation peak-to-peak voltage was 10 mV and the modulation frequency was 317 Hz. The second derivative d^2I/dV^2 spectra were obtained mathematically from the dI/dV data. The bias voltage (V) was defined with respect to the lower CMS electrode, i.e., electrons tunnel from the lower CMS electrode to the upper CMS electrode at a positive V.

III. EXPERIMENTAL RESULTS

Figure 1(a) shows a cross-sectional high-resolution transmission electron microscope lattice image of a CMS/MgO (2.0 nm)/CMS MTJ layer structure with T_a of 550 °C. This image clearly shows that all layers of CMS/MgO/CMS trilayer were grown epitaxially and were single crystalline. It also shows that both extremely smooth and abrupt interfaces

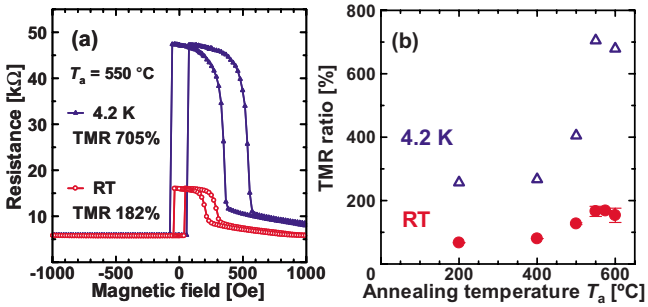

FIG. 2. (Color online) (a) Typical TMR curves at RT and 4.2 K for a Co_2MnSi/MgO (2.7 nm)/Co_2MnSi MTJ fabricated with T_a (the temperature for annealing the MTJ layer structure just after depositing the upper CMS electrode) of 550 °C. The junction size was $10 \times 10\ \mu m^2$. The bias voltage was 1 mV at 4.2 K and 5 mV at RT. (b) TMR ratios at RT and 4.2 K for Co_2MnSi/MgO/Co_2MnSi MTJs as a function T_a.

were formed. Figures 1(b) and 1(c) show microbeam electron diffraction patterns for the upper and lower CMS electrodes, respectively. In both patterns, 111 diffraction spots, which are specific to the $L2_1$ structure, in addition to 002 diffraction spots, were observed, and thus showed that both the lower and upper CMS electrodes had the $L2_1$ structure.

Figure 2(a) shows typical TMR curves at RT and 4.2 K for a fully epitaxial CMS/MgO (2.7 nm)/CMS MTJ that was fabricated with T_a of 550 °C. The applied bias voltage was 1 mV at 4.2 K and 5 mV at RT. The MTJ demonstrated high TMR ratios of 182% at RT and 705% at 4.2 K. At both RT and 4.2 K the TMR ratio of the fully epitaxial MTJs increased significantly with increasing T_a from 400 °C to 550–600 °C [Fig. 2(b)]. MTJs fabricated with T_a of 550–600 °C showed TMR ratios around 700% at 4.2 K and 180% at RT and MTJs fabricated with T_a between 200 and 400 °C showed TMR ratios around 270% at 4.2 K and 80% at RT.

Figure 3 shows typical dI/dV ($=G$) versus V characteristics (G spectra) and corresponding d^2I/dV^2 versus V characteristics (d^2I/dV^2 spectra) for the parallel (P) and antiparallel (AP) magnetization configurations at 4.2 K, which were obtained from a CMS/MgO/CMS MTJ that was fabricated with T_a of 600 °C and showed high TMR ratios of 679% at 4.2 K and 176% at RT. The inset of Fig. 3(a) shows the normalized dI/dV spectra for P and AP (G_P and G_{AP} spectra, respectively), where G_P and G_{AP} are normalized by their respective values at $V=0$. A marked increase in G_{AP} with increasing V was clearly observed in the small bias region of $|V| \leq 70$ mV at 4.2 K [Fig. 3(a)]. This clear structure in the G_{AP} spectrum almost disappeared at RT. Corresponding to the marked increase in G_{AP} for $|V| \leq 70$ mV, pronounced peak structures in the d^2I/dV^2 spectrum for AP with peaks at ± 4 mV were observed [Fig. 3(b)]; these indicated magnon excitation in the collector electrode (i.e., the lower CMS electrode for $V<0$ and the upper CMS electrode for $V>0$) caused by tunnel electrons with excess energies above E_F (i.e., hot electrons).[19] Beyond $|V| \sim 70$ mV, G_{AP} showed a weak dependence on V for $|V| \leq 0.20$ V, and G_{AP} increased sharply at almost equal characteristic voltages V_{C1} of $\sim \pm 0.20$ V for both polarities.

On the other hand, the overall G_P spectrum for the MTJ

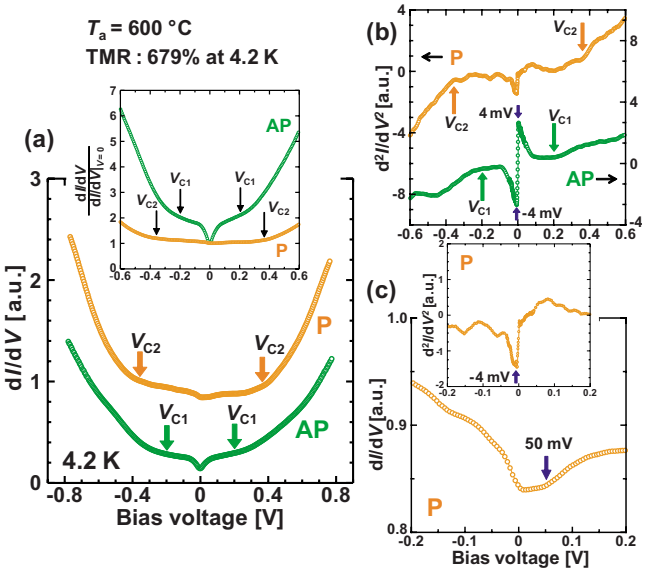

FIG. 3. (Color online) Typical dI/dV (=G) vs V characteristics (G spectra) and corresponding d^2I/dV^2 spectra at 4.2 K for the P and AP magnetization configurations obtained from a Co_2MnSi/MgO (2.2 nm)/Co_2MnSi MTJ (T_a of 600 °C) that exhibited TMR ratios of 679% at 4.2 K and 176% at RT. The bias voltage (V) was defined with respect to the lower Co_2MnSi electrode: (a) G_P and G_{AP} spectra. The inset shows corresponding normalized G_P and G_{AP} spectra, where G_P and G_{AP} are normalized by their respective values at V=0. (b) d^2I/dV^2 spectra for P and AP. The origin of the d^2I/dV^2 values for P is offset from that for AP for clarity. The d^2I/dV^2 values for P and AP refer to the left-side and right-side axes, respectively. (c) Magnification of the G_P spectra shown in (a) for -0.2 V$<V<$0.2 V. The inset shows the magnification of the d^2I/dV^2 spectra for P shown in (b) for -0.2 V$<V<$0.2 V.

with T_a of 600 °C [MTJ (600 °C)] showed a very weak dependence on V up to ±0.36 V [Fig. 3(a)]. This feature can be more clearly seen in the normalized G_P spectrum [inset of Fig. 3(a)]. G_P also increased sharply at almost equal characteristic voltages V_{C2} of ±0.36 V for both polarities [Fig. 3(a)]. These V_{C1} and V_{C2} values were determined from the corresponding, more distinct, structures in the respective d^2I/dV^2 spectra for P and AP [Fig. 3(b)].

Even though the overall G_P spectrum showed a very weak dependence on V up to V of ±0.36 V, a more detailed examination revealed that the G_P spectrum at a small bias, especially for $|V|<50$ mV, was notably asymmetric regarding the bias polarity [Fig. 3(c)]. The G_P spectrum for $V<0$, where electrons tunnel from the upper CMS to the lower CMS, showed a clear increase with increasing V up to ~ -30 mV, but the G_P spectrum for $V>0$, where electrons tunnel from the lower CMS to the upper CMS, was almost completely independent of V up to $V\sim 50$ mV (i.e., the d^2I/dV^2 values were nearly zero for this region). The corresponding d^2I/dV^2 spectrum for P demonstrated a clear peak structure with a peak at -4 mV only for $V<0$ [inset of Fig. 3(c)], indicating magnon excitation caused by tunnel electrons with excess energies for P and $V<0$.

Figure 4 shows typical G and d^2I/dV^2 spectra for P and AP at 4.2 K, which were obtained from a CMS/MgO/CMS MTJ that was fabricated with T_a of 400 °C and showed lower TMR ratios of 267% at 4.2 K and 80% at RT. A marked increase in G_{AP} with increasing V was observed in the small bias region of $|V|\leq 70$ mV at 4.2 K [Fig. 4(a)] for

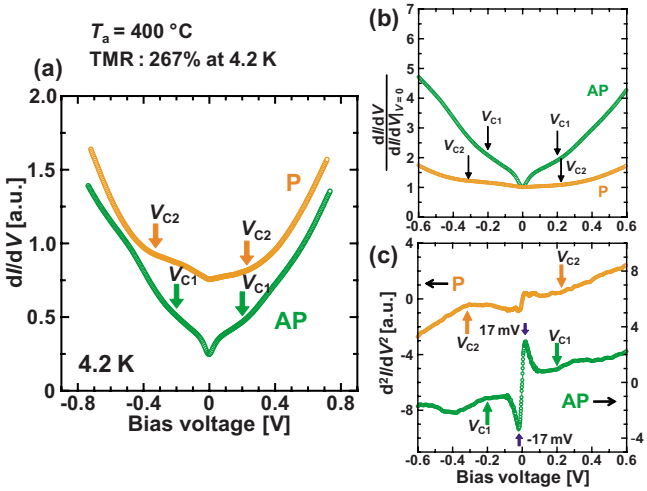

FIG. 4. (Color online) Typical G spectra and corresponding d^2I/dV^2 spectra at 4.2 K for P and AP obtained from a Co_2MnSi/MgO (2.0 nm)/Co_2MnSi MTJ (T_a of 400 °C) that exhibited TMR ratios of 267% at 4.2 K and 80% at RT. (a) G_P and G_{AP} spectra. (b) Corresponding normalized G_P and G_{AP} spectra, where G_P and G_{AP} are normalized by their respective values at V =0. (c) d^2I/dV^2 spectra for P and AP. The origin of the d^2I/dV^2 values for P is offset from that for AP for clarity. The d^2I/dV^2 values for P and AP refer to the left-side and right-side axes, respectively.

the MTJ with T_a of 400 °C [MTJ (400 °C)], and this increase was similar to the increase observed for the MTJ (600 °C). Corresponding to the marked increase in G_{AP} for $|V|\leq 70$ mV, pronounced peak structures in the d^2I/dV^2 spectrum for AP with peaks at ±17 mV were observed [Fig. 4(c)]. Beyond $|V|\sim 70$ mV, however, G_{AP} showed moderate increases with increasing V up to $|V|\leq 0.20$ V for both polarities [Figs. 4(a) and 4(b)], which is in contrast to the weak dependence of G_{AP} for these regions observed for the MTJ (600 °C). Beyond these regions, G_{AP} increased sharply at almost equal characteristic voltages V_{C1} of $\sim\pm 0.20$ V for both polarities. Note that these V_{C1} values were almost equal to those for the MTJ (600 °C). The G_P spectrum for the MTJ (400 °C), on the other hand, exhibited sharp increases at characteristic voltages V_{C2+} of 0.22 V for $V>0$ and V_{C2-} of -0.30 V for $V<0$, and these V_{C2} values were smaller than those for the MTJ (600 °C) (±0.36 V).

IV. DISCUSSION

A. Half-metal gap structures deduced from spin-dependent *dI/dV* spectra

We will now discuss the tunneling processes responsible for the observed G spectra for P and AP and consider the related spin-dependent electronic structure in the lower and upper CMS electrodes. First, we consider the observed clear increases in G_{AP} and G_P at the characteristic voltages of V_{C1} and V_{C2}, respectively. These sharp increases suggest the existence of the minority-spin band gap (half-metal gap) for the lower and upper CMS electrodes. Given this guideline, we will discuss the tunneling process for AP and $V>0$ first. As shown in Fig. 5(a), there are two possible tunneling paths: one from the minority-spin (m-spin) valence band in the lower CMS to the unoccupied majority-spin (M-spin) band above E_F in the upper CMS [path-a in Fig. 5(a)], and the

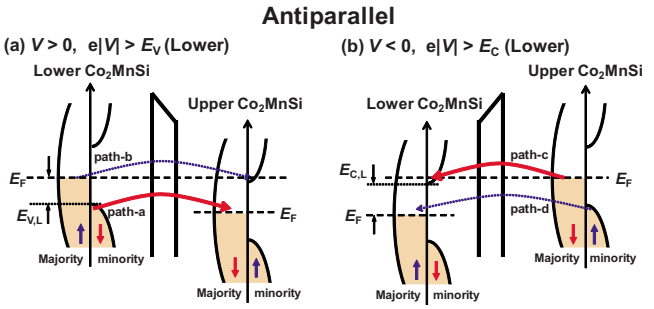

FIG. 5. (Color online) Schematic diagrams of the respective band-to-band tunneling processes in a CMS/MgO/CMS MTJ for the AP configuration at (a) $V>0$ and (b) $V<0$. The suffixes L in $E_{V,L}$ and $E_{C,L}$ represent E_V and E_C for the lower CMS electrode, respectively. We ascribe the sharp increase in G_{AP} at a characteristic voltage V_{C1} for $V>0$ ($V<0$) to tunneling path-a (path-c) in (a) and (b).

other from the M-spin band in the lower CMS to the unoccupied m-spin conduction band above E_F in the upper CMS [path-b in Fig. 5(a)]. Here we assume that the valence-band and conduction-band edges of the lower CMS electrode were more abrupt than those of the upper CMS electrode. We thus ascribe the sharp increase in G_{AP} at V_{C1+} (V_{C1} for $V>0$) to the opening of path-a shown in Fig. 5(a). This results in a correspondence relation between V_{C1+} and E_V: $E_V=eV_{C1+}$, where E_V is the energy difference from E_F to the top of the m-spin valence band located below E_F. Accordingly, we estimated the value of E_V for the lower CMS to be 0.20 eV for the MTJ (600 °C) and for the MTJ (400 °C).

Making the same assumption, we ascribe the sharp increase in G_{AP} at V_{C1-} (V_{C1} for $V<0$) to the opening of the tunneling path from the M-spin band in the upper CMS to the unoccupied m-spin conduction band in the lower CMS electrode [path-c in Fig. 5(b)], rather than the opening of the tunneling path from the m-spin valence band in the upper CMS to the M-spin band in the lower CMS [path-d in Fig. 5(b)]. This results in a correspondence relation between V_{C1-} and E_C: $E_C=e|V_{C1-}|$, where E_C is the energy difference from E_F to the bottom of the m-spin conduction band located above E_F. Accordingly, we estimated the value of E_C for the lower CMS to be 0.20 eV for the MTJ (600 °C) and for the MTJ (400 °C). Thus, the G_{AP} spectra of CMS/MgO/CMS MTJs directly revealed a nearly equal value of 0.20 eV for both E_V and E_C of the lower CMS electrodes of MTJs fabricated with T_a of either 600 or 400 °C. This results in a half-metal gap ($E_g=E_V+E_C$) of 0.40 eV and an important finding that the E_F position was near the middle of the half-metal gap for the lower CMS electrodes of the MTJs fabricated with T_a of either 600 or 400 °C. The obtained equal values of the half-metal gaps for the lower CMS electrodes are reasonable, given that the lower CMS electrodes were both *in situ* annealed at 600 °C just after the lower electrode was deposited at RT. This supports the validity of assuming that the valence-band and conduction-band edges of the lower CMS electrode were more abrupt than those of the upper CMS electrode.

Next we will discuss the tunneling process responsible for the pronounced increase seen for the P configuration. The distinct increases in G_P were observed at higher characteristic voltages than were the increases in G_{AP}, indicating that the increases in G_P are due to the opening of the tunneling path from the m-spin valence band to the unoccupied m-spin conduction band. Thus, the sharp increase in G_P at V_{C2} for $V>0$ ($V<0$) is attributed to the opening of a tunneling path from the m-spin valence band of the lower (upper) CMS to the unoccupied m-spin conduction band of the upper (lower) CMS, resulting in a representation of $eV_{C2+}=E_V$ (lower CMS)$+E_C$ (upper CMS), where V_{C2+} is V_{C2} for $V>0$, and $e|V_{C2-}|=E_V$ (upper CMS)$+E_C$ (lower CMS), where V_{C2-} is V_{C2} for $V<0$. We already estimated the values of E_V (lower CMS) and E_C (lower CMS) for MTJs (600 °C) and for MTJs (400 °C). Accordingly, we obtained the values of E_V (upper CMS) and E_C (upper CMS) from the values of V_{C2-} and V_{C2+}. Thus obtained values of E_V (upper CMS) and E_C (upper CMS) for the MTJ (600 °C) were both 0.16 eV, resulting in a half-metal gap of 0.32 eV for the upper CMS electrode in the MTJ (600 °C) and also resulting in the E_F position being near the middle of the half-metal gap. The E_g value of 0.32 eV for the upper CMS electrode was smaller than the 0.40 eV obtained for the lower CMS electrode. On the other hand, the obtained values of E_V (upper CMS) and E_C (upper CMS) for the MTJ (400 °C) were respectively 0.10 and 0.02 eV, resulting in a small E_g (0.12 eV). Compared to the almost constant E_g of 0.40 eV for the lower CMS electrode in the MTJ annealed at either 600 or 400 °C, the difference between E_g for the upper CMS of the MTJ (600 °C) and that for the upper CMS of the MTJ (400 °C) (i.e., the difference between 0.32 and 0.12 eV) is notable.

B. Tunneling mechanism within a small bias region

We will now discuss the G spectra for P and AP within a small bias region of $|V|<100$ mV. We will first examine the G_P spectra. G_P spectra for MTJs with T_a of 600 and 400 °C in both cases showed asymmetric behavior at a small bias, in particular for $|V|\leq 50$ mV, relative to the bias polarity as shown in Figs. 3 and 4, and the asymmetric behavior was more pronounced for MTJs (600 °C). This asymmetric behavior of the G_P spectra is the key to clarifying the spin-dependent electronic structure of the lower and upper CMS electrodes with regard to the half-metal gap as well as the possible existence of interface states and/or residual states located around E_F in the m-spin band gap.[20] Here, we will examine the G_P spectrum of the MTJ (600 °C) that showed more pronounced asymmetric behavior compared to that of the MTJ (400 °C). We proposed a model of spin-dependent electronic structures for the lower and upper CMS electrodes to explain the observed G and d^2I/dV^2 spectra as schematically illustrated in Fig. 6 (Ref. 20). The observed features for P can reasonably be explained by assuming (1) the existence of interface states around E_F in the m-spin band gap in the interfacial region of the lower CMS electrode facing a MgO barrier and (2) the existence of residual states around E_F in the m-spin band gap in the bulk region of the upper CMS in addition to interface states for the upper CMS electrodes. As we described in Sec. III, the overall G_P spectra showed a very weak dependence on V up to V_{C2} of ± 0.36 V in spite of the asymmetric behavior within the small bias region. This

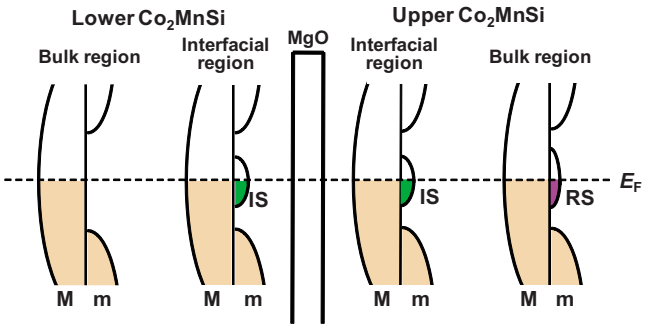

FIG. 6. (Color online) Schematic diagram of a model of spin-dependent electronic structures for the lower and upper CMS electrodes in CMS/MgO/CMS MTJs. Here, IS represents interface states for minority spins and RS represents residual states for minority spins in the bulk region of the upper CMS electrode. *M* and *m* refer to majority and minority spins, respectively.

feature suggests that the tunneling conductance for P is quite high due to coherent tunneling[21,22] from the *M*-spin Δ_1 channel of CMS in CMS/MgO/CMS, which has been theoretically predicted,[23] and so the contribution of tunneling involving the inelastic process in the electrodes would be relatively small. If we take into consideration the monotonic dispersion relation of the energy E versus the wave number k_z along [001] from Γ to X near E_F for CMS,[14,23] it is improbable that the asymmetric behavior observed in the G_P spectrum within the small bias region was due to tunneling from the *M*-spin Δ_1 channel to the *M*-spin Δ_1 channel. Thus, the asymmetric behavior should be attributed to tunneling from *m*-spin channel to *m*-spin channel. According to the analysis provided in Sec. IV A, a tunneling path from the *m*-spin valence band of the upper CMS to the unoccupied *m*-spin conduction band of the lower CMS opened at $V_{C2}=-0.36$ V; this means, it cannot account for the increase in G_P for $V<0$ with increasing V up to -30 mV. Thus, we attributed the observed asymmetric behavior for P within the small V region to tunneling from the *m*- to *m*-spin states, both of which are located around E_F in the *m*-spin band gap. These considerations led us to reasonably assume that (1) residual states with a small density of states exist around E_F in the *m*-spin band gap in the bulk region of the upper CMS electrode and these act as the electron source responsible for the increase in G_P with increasing V up to ~ -30 mV, and (2) there is a negligibly small density of such states for the lower CMS electrode. Furthermore, we assumed the existence of interface states around E_F in the *m*-spin band gap in the interfacial region of the lower CMS electrode facing a MgO barrier as *m*-spin states around E_F. This led us to also assume the existence of such interface states for the upper CMS electrode. The existence of interface states for minority spins around E_F in the interfacial region of CMS electrodes facing a MgO barrier has recently been predicted theoretically through first-principles calculations of electronic structures.[24]

Given the model of the spin-dependent electronic structures for the lower and upper CMS electrodes described above (Fig. 6), the increase in G_P at 4.2 K for $V<0$ up to -30 mV is explained by the following tunneling process. Electrons in residual states existing around E_F in the *m*-spin band gap in the bulk region of the upper CMS are supplied to *m*-spin interface states located around E_F in the interfacial region of the upper CMS, and then tunnel into *m*-spin interface states located around E_F of the lower CMS. This tunneling process cannot contribute to the tunneling conductance without spin-flip scattering in the lower CMS because there is no available state for minority spins around E_F in the bulk region of the lower CMS. Tunnel electrons with excess energies, however, excite magnons in the interfacial region of the lower CMS electrode. The tunneling electrons are then spin-flip scattered to the *M*-spin band in the lower CMS electrode and contribute to the tunnel conductance. This picture combines the concept of electrons tunneling into interface states[18] with that of magnon excitation by hot electrons in the collector electrode,[19] i.e., the lower CMS electrode for $V<0$. On the other hand, the almost complete independence of G_P on positive V up to ~ 50 mV indicates that there was no electron source for *m*-spin states around E_F in the bulk region of the lower CMS, i.e., it indicates that the lower CMS electrode, in contrast to the upper CMS electrode, featured a negligibly small density of residual states around E_F in the *m*-spin band gap in the bulk region. The existence of residual states in the *m*-spin band gap for the upper CMS may be related to a possible lower structural quality of the 5-nm-thick upper CMS thin film that was grown on a 2–3-nm-thick MgO barrier.

The sharp increase in G_{AP} with increasing V in the small bias region of $|V|\leq 70$ mV can be consistently explained with the same model of spin-dependent electronic structures for the lower and upper CMS electrodes as follows: (1) Electrons tunnel from the *M*-spin band of the upper CMS to *m*-spin interface states of the lower CMS (here, we consider a tunneling process for $V<0$). (2) Tunnel electrons excite magnons in the interfacial region due to their excess energies above E_F in the lower CMS and simultaneously electrons are spin-flip scattered to the *M*-spin band in the lower CMS, contributing to the marked increase in G_{AP}. The tunneling process for $V>0$ is essentially the same.

The moderate increases in G_{AP} with increasing V for the voltage range of 70 mV$<|V|<$0.20 V for both polarities observed for the MTJ (400 °C) (Sec. III) can be understood by assuming (1) a higher density of residual states existing around E_F in the *m*-spin band gap in the bulk region of the upper CMS electrode and (2) a wider energy range around E_F of such states for the MTJ (400 °C). These characteristics of residual states probably occurred simultaneously with the shrinkage of E_g for the upper CMS in the MTJ (400 °C). A higher density of residual states for minority spins around E_F in the bulk region of the upper CMS is consistent with the lower TMR ratios observed for the MTJ (400 °C).

The T dependence of the tunneling resistances differed for P and AP (R_P and R_{AP}, respectively) of the CMS/MgO/CMS MTJs in that R_{AP} decreased with increasing T from 4.2 K to RT, while R_P was almost completely independent of T from 4.2 K to RT.[20] It is clear that the R_{AP} dependence on T determined the T dependence of the TMR ratio. With increasing T, spin-flip scattering of electrons in the emitter electrode from the *M*-spin band to *m*-spin interface states existing around E_F in the half-metal gap could be caused by thermally excited magnons, and this would enable tunneling from *m*-spin interface states around E_F in the emitter to the

M-spin band of the collector electrode, resulting in a tunneling conductance increase for AP. Similarly, with increasing T, spin-flip scattering in the collector electrode from m-spin interface states existing around E_F in the half-metal gap to the M-spin band could be caused by thermally excited magnons, and this would enable tunneling from the M-spin band in the emitter to m-spin interface states around E_F in the collector and subsequent spin-flip scattering to the M-spin band of the collector electrode, resulting in a tunneling conductance increase for AP. This picture was originally discussed by Mavropoulos *et al.*[18] We also ascribe the almost complete independence of R_P with respect to T to the high tunnel conductance for P—to which we also attribute the very weak dependence of G_P on V up to V_{C2} of ± 0.36 V—due to the coherent tunneling contribution from the M-spin Δ_1 channel, i.e., any tunneling conductance increase for P due to a tunneling process involving spin-flip scattering in the electrodes that is caused by thermally excited magnons is relatively small.

Our model for the spin-dependent electronic structure for the lower and upper CMS electrodes and for the spin-dependent tunneling process consistently explains the observed tunneling spectra, including those at both finite and small voltages. This supports the validity of our model for the semiquantitative estimation of the half-metal gap values and for clarifying the critical role of interface states in MTJs with half-metallic electrodes. More appropriately, however, tunneling from the m-spin band to the m-spin band for P and that from the m-spin band to the M-spin band and vice versa for AP should be theoretically treated by taking into account the conservation of the electron wave vector parallel to the plane (coherent tunneling)[21–23] as the first approximation (neglecting defects and inelastic scattering), but under the condition that a finite voltage is applied greater than E_V/e or E_C/e for AP or $(E_V+E_C)/e$ for P for fully epitaxial MTJs with half-metallic CMS electrodes and a MgO barrier. Furthermore, spin-dependent tunneling spectra at a small bias less than E_V/e or E_C/e, taking into consideration (1) tunneling to interface states existing in the m-spin band gap with the framework of coherent tunneling and (2) successive inelastic spin-flip scattering in the collector electrode, should be theoretically treated.

V. CONCLUSION

We investigated spin-dependent electronic structures of CMS electrodes and the key tunneling mechanism in fully epitaxial CMS/MgO/CMS MTJs through tunneling spectroscopy. The dI/dV $(=G)$ spectra for P and AP at 4.2 K at finite voltages clearly showed that lower and upper CMS electrodes in these MTJs featured a half-metallic electronic structure with the E_F position located near the middle of the respective half-metal gaps. We developed a model of the spin-dependent electronic structure for CMS electrodes and a tunneling model that can consistently explain the obtained G_P and G_{AP} spectra at 4.2 K at both finite voltages and small voltages of $|V|<100$ mV. We found strong evidence that interface states existed in the interfacial region of CMS electrodes facing a MgO barrier, as well as evidence of residual states in the bulk region of upper CMS electrodes, in both cases for minority spins around E_F, and demonstrated the critical role played by interface states with regard to spin-dependent tunneling in half-metallic CMS-based MTJs.

ACKNOWLEDGMENTS

The authors are grateful to Professor Masafumi Shirai and Assistant Professor Yoshio Miura for their enlightening discussions. This work was partly supported by a Grant-in-Aid for Scientific Research (A) (Grant No. 20246054) and a Grant-in-Aid for Scientific Research on Priority Area "Creation and control of spin current" (Grant No. 19048001) from the MEXT, Japan, and by the Strategic International Cooperative Program, JST. T. I. was also supported by a Research Fellowship for Young Scientists from the JSPS.

[1] S. A. Wolf, D. D. Awschalom, R. A. Buhrman, J. M. Daughton, S. von Molnár, M. L. Roukes, A. Y. Chtchelkanova, and D. M. Treger, Science **294**, 1488 (2001).
[2] R. A. de Groot, F. M. Mueller, P. G. van Engen, and K. H. J. Buschow, Phys. Rev. Lett. **50**, 2024 (1983).
[3] S. Kämmerer, A. Thomas, A. Hütten, and G. Reiss, Appl. Phys. Lett. **85**, 79 (2004).
[4] Y. Sakuraba, M. Hattori, M. Oogane, Y. Ando, H. Kato, A. Sakuma, T. Miyazaki, and H. Kubota, Appl. Phys. Lett. **88**, 192508 (2006).
[5] N. Tezuka, N. Ikeda, S. Sugimoto, and K. Inomata, Jpn. J. Appl. Phys., Part 2 **46**, L454 (2007).
[6] T. Ishikawa, T. Marukame, H. Kijima, K.-i. Matsuda, T. Uemura, M. Arita, and M. Yamamoto, Appl. Phys. Lett. **89**, 192505 (2006).
[7] T. Marukame, T. Ishikawa, S. Hakamata, K.-i. Matsuda, T. Uemura, and M. Yamamoto, Appl. Phys. Lett. **90**, 012508 (2007).
[8] S. Hakamata, T. Ishikawa, T. Marukame, K.-i. Matsuda, T. Uemura, M. Arita, and M. Yamamoto, J. Appl. Phys. **101**, 09J513 (2007).
[9] M. Yamamoto, T. Marukame, T. Ishikawa, K.-i. Matsuda, and T. Uemura, Adv. Solid State Phys. **47**, 105 (2008).
[10] T. Ishikawa, S. Hakamata, K.-i. Matsuda, T. Uemura, and M. Yamamoto, J. Appl. Phys. **103**, 07A919 (2008).
[11] S. Tsunegi, Y. Sakuraba, M. Oogane, K. Takanashi, and Y. Ando, Appl. Phys. Lett. **93**, 112506 (2008).
[12] K. Yakushiji, K. Saito, S. Mitani, K. Takanashi, Y. K. Takahashi, and K. Hono, Appl. Phys. Lett. **88**, 222504 (2006).
[13] S. Ishida, S. Fujii, S. Kashiwagi, and S. Asano, J. Phys. Soc. Jpn. **64**, 2152 (1995).
[14] S. Picozzi, A. Continenza, and A. J. Freeman, Phys. Rev. B **66**, 094421 (2002).
[15] I. Galanakis, P. H. Dederichs, and N. Papanikolaou, Phys. Rev. B **66**, 174429 (2002).
[16] P. J. Webster, J. Phys. Chem. Solids **32**, 1221 (1971).
[17] L. Chioncel, Y. Sakuraba, E. Arrigoni, M. I. Katsnelson, M. Oogane, Y. Ando, T. Miyazaki, E. Bruzo, and A. I. Lichtenstein, Phys. Rev. Lett. **100**, 086402 (2008).
[18] Ph. Mavropoulos, M. Ležaić, and S. Blügel, Phys. Rev. B **72**, 174428 (2005).
[19] S. Zhang, P. M. Levy, A. C. Marley, and S. S. P. Parkin, Phys. Rev. Lett. **79**, 3744 (1997).
[20] T. Ishikawa, N. Itabashi, T. Taira, K.-i. Matsuda, T. Uemura, and M. Yamamoto, Appl. Phys. Lett. **94**, 092503 (2009).
[21] W. H. Butler, X.-G. Zhang, T. C. Schulthess, and J. M. MacLaren, Phys. Rev. B **63**, 054416 (2001).
[22] J. Mathon and A. Umerski, Phys. Rev. B **63**, 220403 (2001).
[23] Y. Miura, H. Uchida, Y. Oba, K. Nagao, and M. Shirai, J. Phys.: Condens. Matter **19**, 365228 (2007).
[24] Y. Miura, H. Uchida, Y. Oba, K. Abe, and M. Shirai, Phys. Rev. B **78**, 064416 (2008).